Eur Radiol (2014) 24:1357–1365
DOI 10.1007/s00330-014-3116-y

MUSCULOSKELETAL

Intraosseous rotation of the scaphoid: assessment by using a 3D CT model—an anatomic study

Gernot Schmidle · Michael Rieger · Andrea Sabine Klauser · Michael Thauerer · Romed Hoermann · Markus Gabl

Received: 8 November 2013 / Revised: 27 January 2014 / Accepted: 5 February 2014 / Published online: 6 March 2014

Abstract
Objectives The purpose of this study was to assess intraosseous rotation as the third dimension of scaphoid anatomy on a 3D CT model using common volume rendering software to impact anatomical reconstruction of scaphoid fractures.
Methods CT images of 13 cadaver wrist pairs were acquired. Reference axes for the alignment of distal and proximal scaphoid poles were defined three-dimensionally. Two methods for rotation measurement—the reference axis method (RAM) and the scapho-trapezio-trapezoidal joint method (STTM)—were developed and compared by three independent observers.
Results Rotation measured by the RAM averaged 66.9°±7 for the right and 67.2°±5.8 for the left wrists. Using the STTM there was a mean rotation of 68.6°±6.6 for the right and 68.6° ±6.8 for the left wrists. The overall results showed a significant variability of the measured values between different specimens ($P<0.05$). There was no significant difference between left and right wrists of the same specimen, neither for the RAM ($P=0.268$) nor for the STTM ($P=0.774$). Repeatability coefficients between the observers were low, indicating good repeatability.
Conclusions The presented methods are practical tools to quantify intraosseous rotation between distal and proximal scaphoid poles using common volume rendering software. For clinical application the opposite side provides the best reference values to assess malrotation in scaphoid fracture cases.
Key points
- *Scaphoid intraosseous rotation can be measured using common volume rendering software.*
- *The opposite uninjured side provides good reference values for rotation measurement.*
- *Assessment of malrotation may impact anatomical reconstruction of scaphoid fractures.*

Keywords Scaphoid bone · Rotation · Three-dimensional imaging · Computed tomography · Anatomy

Abbreviations and acronyms

DISI	dorsal intercalated segment instability
RAM	reference axis method
STTM	scapho-trapezio-trapezoidal joint method
TT	trapezio-trapezoidal

Introduction

The scaphoid plays a central role in carpal kinematics. It is prone to injury and reported to be the most frequently fractured carpal bone [1]. The complex shape of the scaphoid and its tenuous blood supply increase the risk of non-union that can lead to advancing osteoarthritis of the wrist [2].

Malalignment of the fracture fragments additionally reduces the small contact surface and can lead to gapping,

G. Schmidle (✉) · M. Gabl
Department of Trauma Surgery, Medical University Innsbruck, Anichstraße 35, 6020 Innsbruck, Austria
e-mail: gernot.schmidle@uki.at

M. Rieger
Department of Radiology, Regional Hospital Hall, Milser Straße 10, 6060 Hall in Tirol, Austria

A. S. Klauser · M. Thauerer
Department of Radiology, Medical University Innsbruck, Anichstraße 35, 6020 Innsbruck, Austria

R. Hoermann
Department of Anatomy, Histology and Embryology–Division of Clinical and Functional Anatomy, Medical University Innsbruck, Muellerstraße 59, 6020 Innsbruck, Austria

increasing the risk of non-union [3]. Gaps of more than 1 mm and angular deformities with dorsal intercalated segment instability (DISI) are seen as an indication for surgery [4–6].

Besides these two-dimensionally assessable fracture patterns, rotational malalignment between scaphoid fracture fragments may alter carpal kinematics. This has already been shown for carpal ligament injuries [7] as well as for scaphoid non-unions [8, 9].

In articular fractures, exact anatomical reconstruction is a general goal of treatment to avoid long-term consequences of osteoarthritis and pain [10]. Therefore exact analysis of the intraosseous malposition is needed.

Fracture gaps and angular deformities in the sagittal and coronal plane can be well demonstrated and measured with 2D CT imaging [5, 11, 12]. Intraosseous rotation as the third dimension of malposition can be identified using three-dimensional image-fusion technology [8, 9, 13–15].

Image-fusion technology provides with exact measurement values but is time consuming and requires special software equipment not available in most trauma centres [16, 17].

The purpose of this cadaver study was to develop a measurement technique to assess intraosseous rotation of the scaphoid for daily clinical use, based on surface landmarks on a 3D CT model using common volume rendering software. Wrist pairs were used to check if the measurement values of the opposite side could serve as a reference for the assessment of malrotation in scaphoid fracture cases.

Materials and methods

All cadavers were dedicated to human studies according to the last will of the donors.

To define reproducible surface landmarks and reference axes, CT images of 26 cadaver wrists (13 wrist pairs) were acquired using a standardized positioning device. The wrist was fixed in neutral position. The thumb was positioned in 30° radial abduction and 30° volar abduction in relation to the second metacarpal bone. This position is equivalent to the thumb spica cast used for scaphoid fracture treatment.

All CT images were acquired with a 64-detector row MDCT (LightSpeed™ VCT, GE, Milwaukee) using a standard bone protocol with a slice thickness of 0.625 mm and acquisition parameters of 100 kV and 100 mAs. The obtained source images were transferred to a 3D rendering workstation

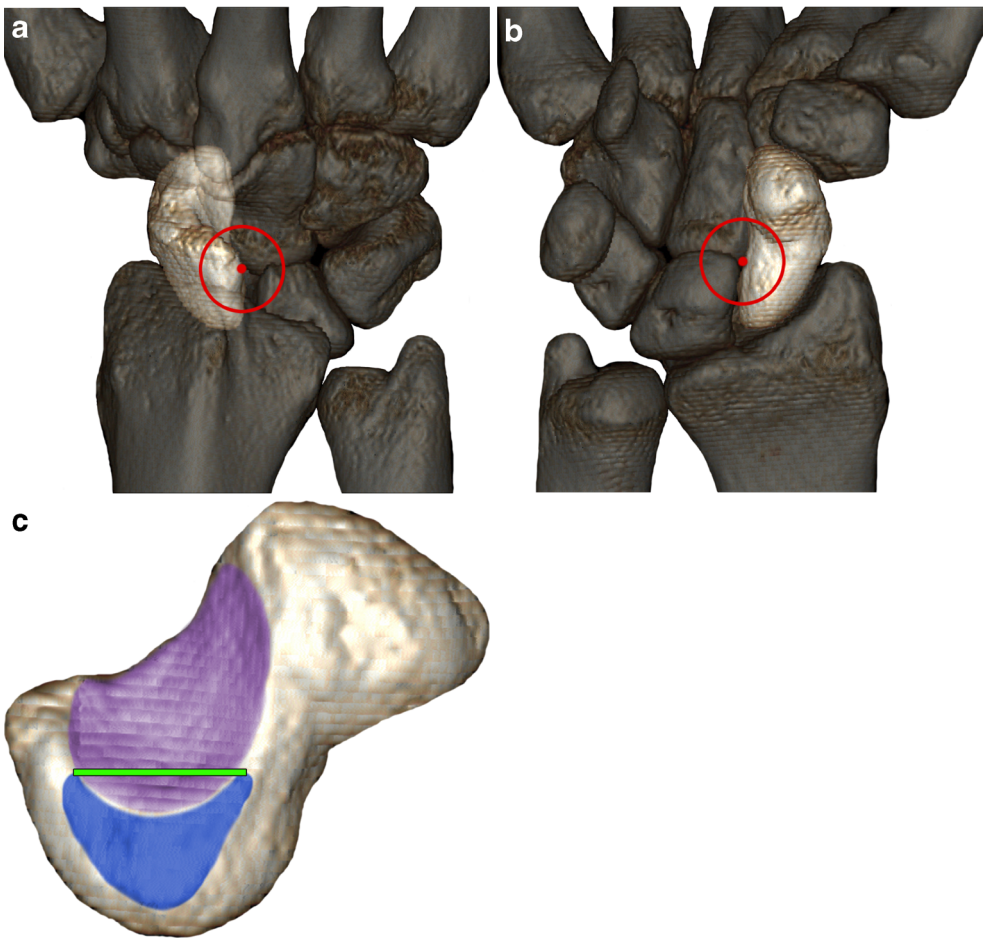

Fig. 1 3D reconstruction of a right wrist **a** in a dorsal view with the most distal dorsal edge of the lunate facet marked with a *red dot* and **b** in a volar view with the most distal volar edge of the lunate facet marked with a *red dot*. **c** The proximal rotational axis (*green line*) is shown in a view from the ulnar

(HP Workstation xw8000) running Advantage Windows software (Advantage Windows 4.6, GE Healthcare).

For the further processing and measurements, the Volume Viewer 3.1 (GE Healthcare) was used. It provides several working surfaces where the data are displayed simultaneously in different views (3D volume rendering reconstructions and 2D reformations in different planes).

In the first step, a 3D volume rendering model of the wrist bones was created. Then the scaphoid was segmented. Two reference axes for the rotational alignment of the scaphoid poles were defined, and a measurement view was set three-dimensionally. On this view the measurement of the angle between the rotational axes was taken two-dimensionally. The measurement values were compared between left and right wrists of the same cadaver and between different cadavers. Three different observers (one orthopaedic surgeon, one senior radiology resident, and one research assistant of the institute of anatomy who were blinded to each other's results) performed the measurements. The observers were instructed and had the possibility to practice the methods on the basis of case examples. The time needed for the measurements was recorded.

Proximal rotational axis

On the ulnar side of the scaphoid there are two articular facets. The proximal smaller facet articulates with the lunate and is flattened to a slightly convex form (Fig. 1c, blue area). The distal larger facet, together with the lunate, forms a concave cavity for the capitate head (Fig. 1c, purple area). The transition zone between these two facets can be visualised three-dimensionally.

The most distal dorsal and volar edges of the articular facet for the lunate were marked (Fig. 1a, b, red dots). The line connecting these marked points was defined as the proximal rotational axis (Fig. 1c, green line). This line served as a reference axis for the rotational alignment of the proximal scaphoid pole.

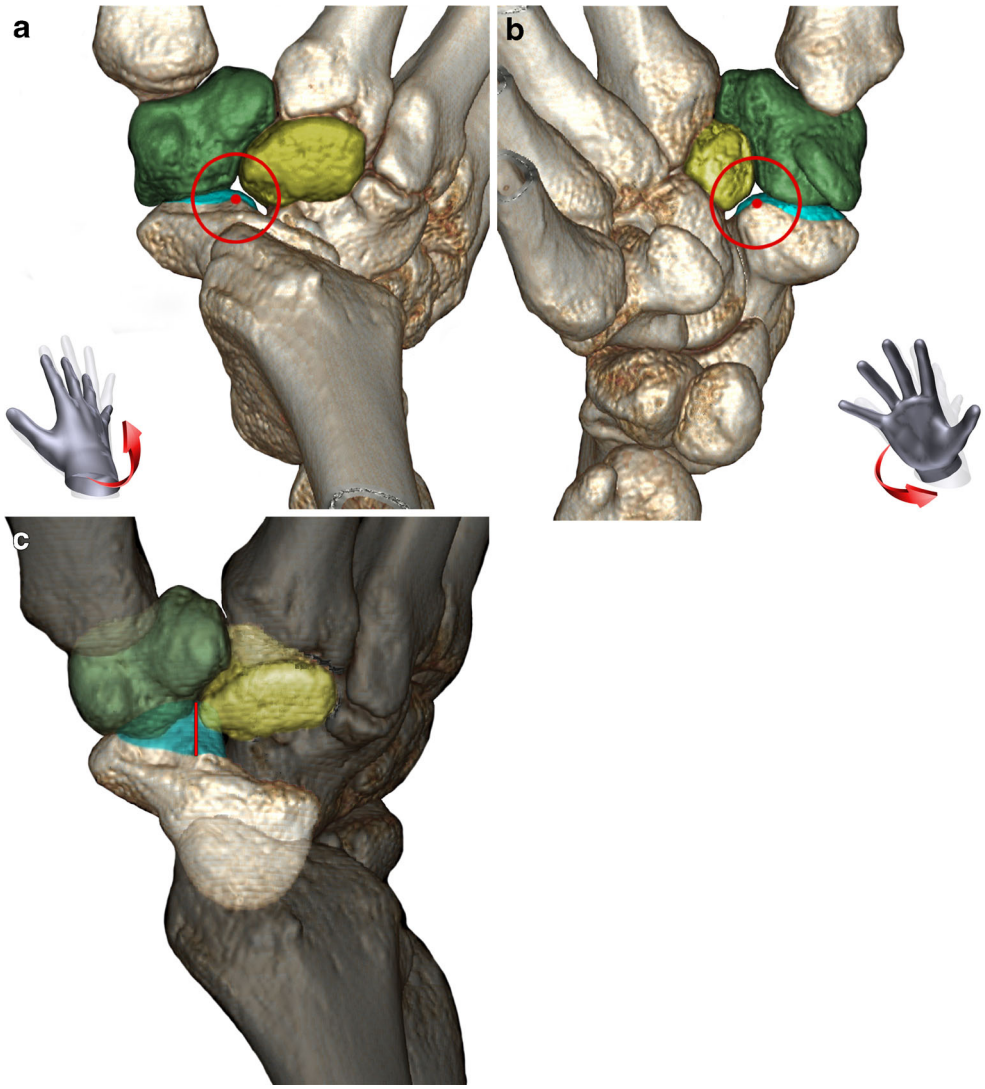

Fig. 2 Shows the trapezium (*green*), the trapezoideum (*yellow*), the distal joint surface of the scaphoid (*turquoise area*) **a** in a view from dorsal and **b** in a view from volar. **c** Shows the distal rotational reference axis (*red line*)

Distal rotational axis

The distal rotational axis was based on the interfacet ridge of the distal joint surface of the scaphoid, which separates the articular facets for trapezium and trapezoideum. It was defined indirectly, because it is not always prominent [18], but oriented in line with the trapezio-trapezoidal (TT) articulation [19].

In a dorsal coronal view, the 3D model was supinated around a vertical axis by approximately 45°. Then it was rotated around a horizontal axis by approximately 30–45° until a free view into the joint gap between trapezium and trapezoideum was achieved (Fig. 2a).

The dorsal edge of the distal joint surface of the scaphoid was marked (Fig. 2a, red dot) in line with the perpendicularly aligned TT joint gap.

In the next step the 3D model was rotated by 180° around a vertical axis (Fig. 2b). The volar edge of the distal joint surface of the scaphoid was marked in the same way (Fig. 2b, red dot).

The resulting line between these points was defined as the distal rotational axis (Fig. 2c, red line). It served as a reference axis for the rotational alignment of the distal scaphoid pole.

Rotation

For the measurement of rotation between these reference axes two different methods were developed to define a viewpoint on the 3D CT model. Out of the defined viewpoints, the rotation angle was measured two-dimensionally.

Reference axis method (RAM)

This method was performed in two steps. In step 1 the proximal rotational axis was positioned as the horizontal axis

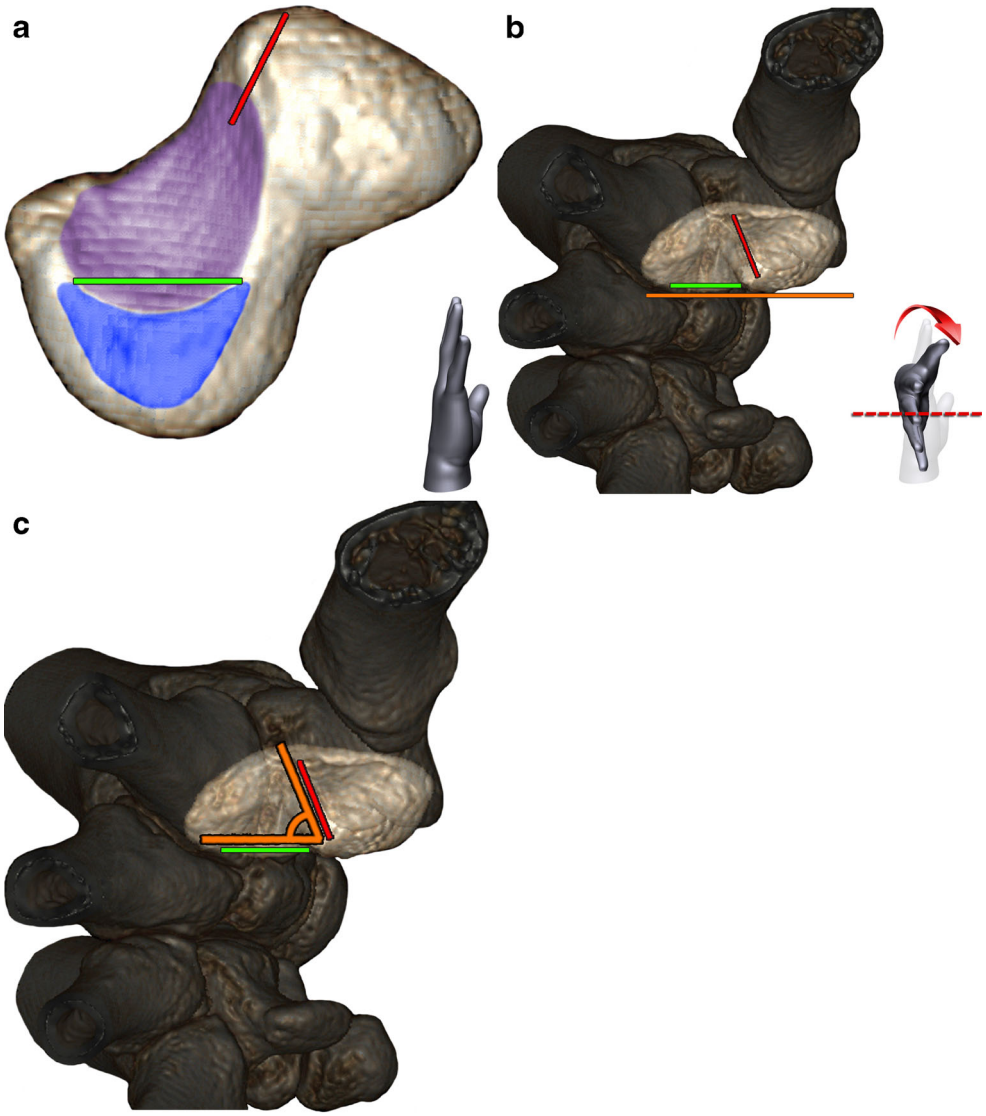

Fig. 3 **a** Right scaphoid in a view from ulnar with the proximal rotational axis (*green line*) and the distal rotational axis (*red line*). **b** View on the scaphoid from distal after rotation around a horizontal axis. Ulnar-sided tangent between the proximal and distal scaphoid poles (*orange line*). **c** Rotation angle (*orange*) between the two reference axes

(Fig. 3a, green line). In step 2, the 3D model was rotated until an imaginary ulnar-sided tangent between the proximal and distal poles of the scaphoid was aligned horizontally (Fig. 3b, orange line). From this viewpoint, the angle between the two rotational reference axes was measured (Fig. 3c).

Scapho-trapezio-trapezoidal joint method (STTM)

The second method is based on the "scaphoid axial view" proposed by Moritomo for visualisation of the scapho-trapezio-trapezoidal joint [19].

In step 1 the 3D model was rotated around a vertical axis until the trapezium and trapezoideum were superimposed in a view from the radial (Fig. 4a).

In step 2 a rotation around a horizontal axis was performed until the proximal joint surfaces of trapezium and trapezoideum were superimposed (Fig. 4b).

In step 3 the 3D model was rotated clockwise until an imaginary ulnar-sided tangent between the scaphoid poles was aligned vertically (Fig. 4c, orange line).

In step 4 the 3D model was rotated distally around a horizontal axis by 90° to obtain the measurement view (Fig. 4d).

Statistical analysis

Statistical analyses were performed using IBM® SPSS® Statistics 20.0 (IBM Corp., USA) and Analyse-it for Microsoft Excel 2.30 (Analyse-it Software, Ltd. http://www.analyse-it.com; 2013). The Kolmogorov–Smirnov test was used for determination of normal distribution. For independent samples, a *t* test was performed. For paired samples, a paired *t* test was used. The relationship between the right and left wrists of the same individual and between the presented measurement methods was analysed by using a Pearson correlation. The (alpha) level of significance was set at $P<0.05$.

For the assessment of repeatability of measurements between the different observers, the repeatability coefficient according to Bland and Altman [20] (1.96 times the standard

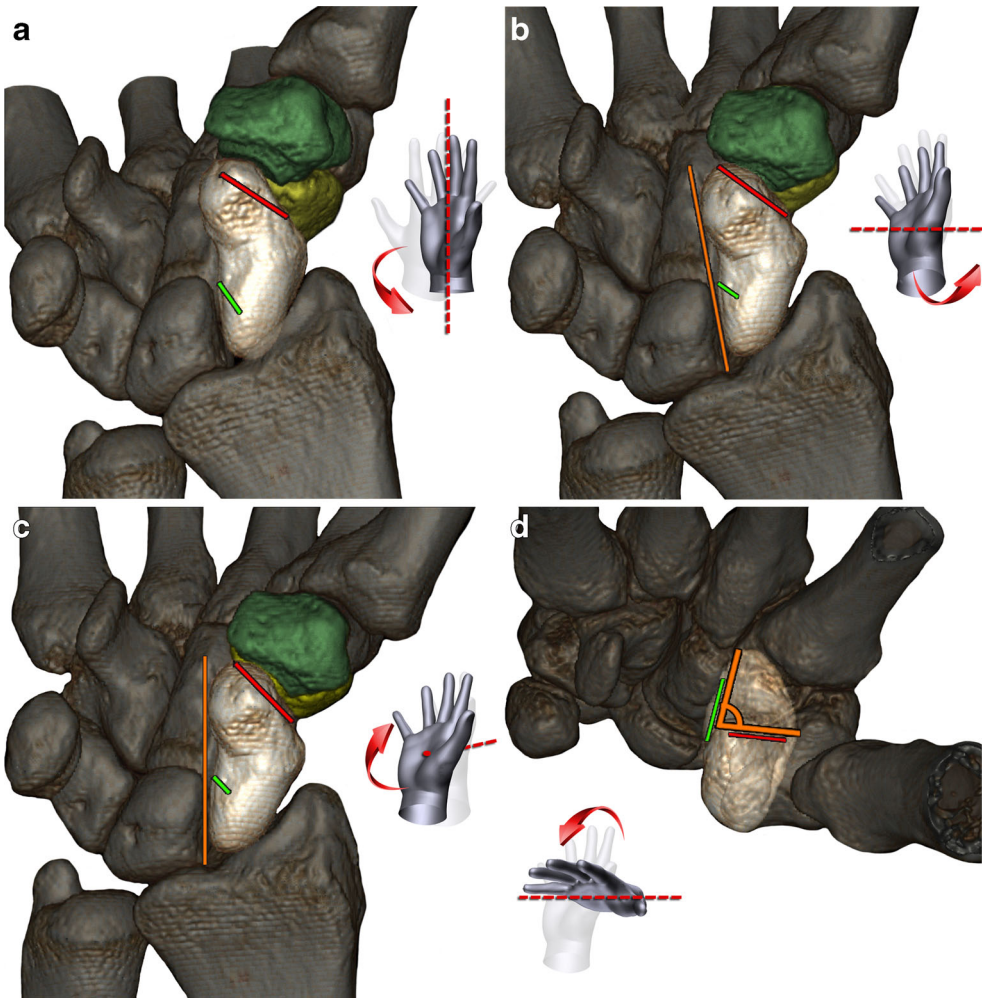

Fig. 4 Right wrist with the proximal rotational axis (*green line*), the distal rotational axis (*red line*), the trapezium (*green*), and the trapezoideum (*yellow*) marked. **a** Position after rotation around a vertical axis, **b** a horizontal axis, and **c** clockwise rotation. **d** Measurement view after rotation by 90°

deviation of the differences between the two measurements) was calculated. Smaller values indicate higher repeatability.

Results

Landmarks and axes were constantly visualised in all cases. Rotation could be measured with both presented methods.

Measurement values for proximal and distal rotational axes and intraosseous rotation of the right and left wrists can be seen in Table 1. Intraosseous rotation of the scaphoid differed significantly between the individuals ($P<0.05$). Between the right and left wrists of the same cadaver specimen no significant differences were found either for the RAM ($P=0.268$) or for the STTM ($P=0.774$). Within the same individual a strong right–left correlation was found for the RAM ($r=0.980$) as well as for the STTM ($r=0.972$). The measurement values obtained by the two presented methods correlated significantly ($P<0.05$) within the group of the right ($r=0.598$) and left wrists ($r=0.645$) respectively.

Repeatability coefficients between the observers were comparable for proximal and distal reference axes, for rotation measurements using the RAM and STTM and for wrist pair difference (Table 2). Repeatability coefficients for STTM were slightly higher, indicating lower repeatability.

The mean time needed for the measurements of one cadaver wrist was 9 min 32 s (range 6 min 32 s–14 min 22 s, standard deviation ±2 min 3 s).

Clinical case

In order to demonstrate the potential clinical value of our findings, a case of a 19-year-old woman is presented. There was a fracture of the right scaphoid with rotational malalignment identified on 3D reconstructions (Fig. 5a). Quantification of intraosseous rotation showed a malrotation of 7.5° (RAM) and 8.2° (STTM) in comparison to the uninjured side. An arthroscopically assisted percutaneous screw fixation was then performed. The malrotation was visualised and corrected under direct arthroscopic vision (Fig. 5b, c).

Discussion

The scaphoid plays a central role in carpal kinematics. It acts as a bridging link or stabilizing rod between the two carpal

Table 1 Measurement values of reference axes and intraosseous rotation

		Right wrists (Different individuals)	Left wrists (Different individuals)	Wrist pair difference (Same individual)
All observers	Proximal rotational axis	12.2±1.2	11.7±1.6	0.7±0.6
	Distal rotational axis	11.2±1.6	11.3±1.8	0.6±0.5
	Rotation – RAM	66.9±7	67.2±5.8	1.4±1
	Rotation – STTM	68.6±6.6	68.6±6.8	1.4±0.8
Observer 1	Proximal rotational axis	12.4±1.3	11.8±1.6	0.7±0.5*
	Distal rotational axis	11.3±1.7	11.3±2.1	0.7±0.6
	Rotation – RAM	66.6±7.5	67±5.5	1.9±1.4
	Rotation – STTM	68.8±6.5	68.7±6.4	1.1±0.7
Observer 2	Proximal rotational axis	12±1.2	11.5±1.6	0.9±0.6
	Distal rotational axis	11±1.5	11.2±1.4	0.5±0.4
	Rotation – RAM	66.9±7	67.5±6.2	1.2±0.6
	Rotation – STTM	68.7±7.7	68.2±7.9	1.7±0.9
Observer 3	Proximal rotational axis	12.2±1.3	11.8±1.7	0.6±0.7
	Distal rotational axis	11.2±1.6	11.4±1.9	0.6±0.4
	Rotation – RAM	67.1±7.1	67.1±6.2	1.3±0.7
	Rotation – STTM	68.5±6	68.8±6.4	1.4±0.6

Data are mean values ± standard deviation

RAM reference axis method, *STTM* scapho-trapezio-trapezoidal joint method

*$p<0.05$

Table 2 Repeatability coefficients

	Proximal rotational axis (mm)	Distal rotational axis (mm)	RAM (°)	STTM (°)	Wrist pair difference RAM (°)	Wrist pair difference STTM (°)
Observer 1 vs. 2	0.82	1.51	2.57	3.88	2.92	1.98
Observer 1 vs. 3	0.63	0.96	2.1	3.63	2.59	1.39
Observer 2 vs. 3	0.9	1.08	2.86	4.63	2.18	2.33

95 % of measurement values are within the range of the repeatability coefficient (= standard deviation × 1.96). Low repeatability coefficients indicate high repeatability; high repeatability coefficients indicate low repeatability

RAM reference axis method, *STTM* scapho-trapezio-trapezoidal joint method

rows. In scaphoid fractures a gap of more than 1 mm and angular deformities are reported to be negative prognostic values for fracture healing [4, 5]. In addition to these fracture patterns, malrotation may lead to midcarpal incongruity with the long-term consequences of osteoarthritis and pain. So the anatomical reconstruction should be an important goal of treatment [2, 3].

Scaphoid fracture displacement is primarily assessed by conventional radiographs. Special scaphoid views are used to visualise the fracture patterns. Even though conventional radiographs are widely used in clinical practice, several studies show their limited worth in the assessment of scaphoid fracture stability and displacement [21–23]. Rotation between fracture fragments can neither be displayed nor measured by conventional radiographs.

Two-dimensional CT imaging improves the assessment of fracture displacement [5, 23, 24]. The extent of displacement as well as angular deformities can reliably be determined and measured [11, 12]. Indirect signs of malrotation can be found on 2D CT reformations but it cannot be quantified.

The complete identification of scaphoid fracture patterns is not possible with two-dimensional imaging alone, so some

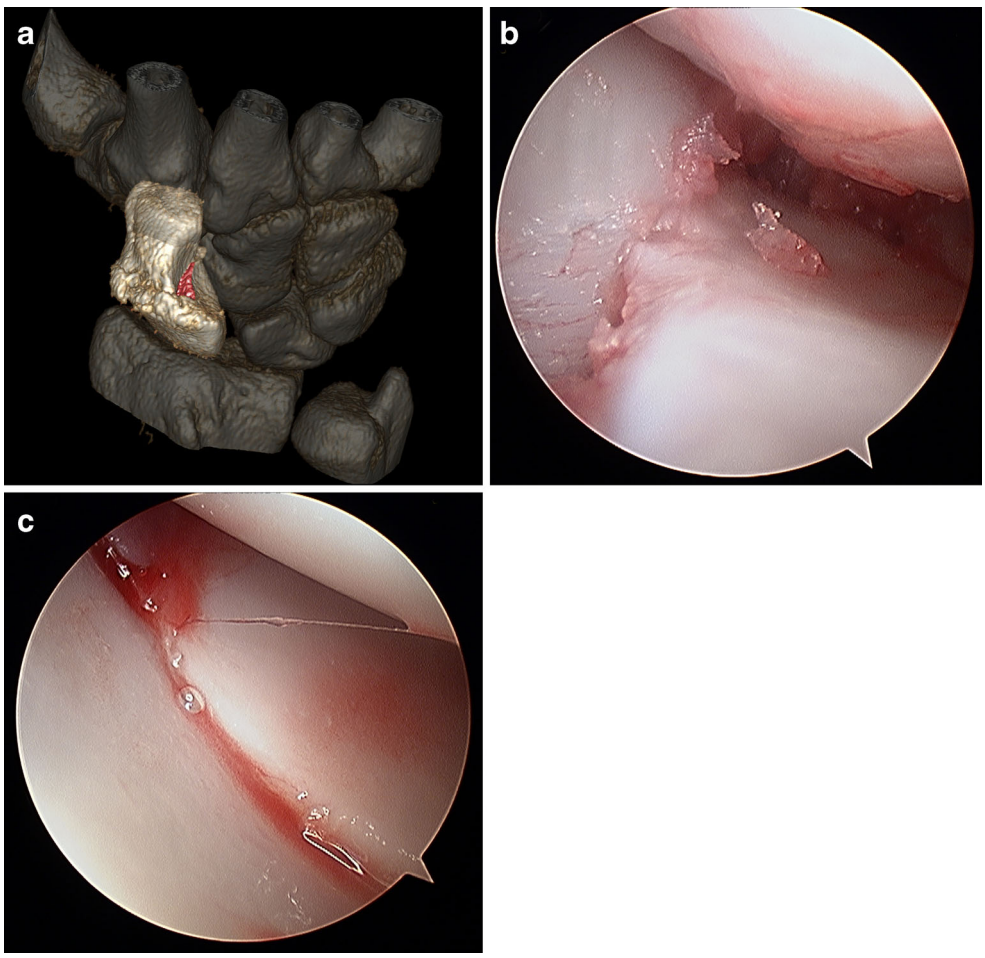

Fig. 5 A 19-year-old woman with an acute scaphoid fracture. **a** 3D model of the wrist with rotational malalignment between the scaphoid fracture fragments (*red area*). **b** Arthroscopic picture of the malrotation through a midcarpal radial (MCR) portal. **c** Arthroscopic picture after reduction

method of three-dimensional reconstruction may be required in clinical practice [17]. The high resolution of modern CT imaging enables high-quality 3D reconstructions and segmentation of small bones such as the scaphoid. Thus nowadays it is possible to assess rotation between scaphoid fracture fragments as the third dimension of malposition.

Reports on 3D measurements of the carpals rely mainly on sophisticated software and time-intensive procedures to assess dislocation. Image-fusion technology achieves high accuracy in the measurement of scaphoid fractures and scaphoid non-unions and their effects on carpal kinematics [8, 9, 13–15]. Therefore the injured side is matched with the mirror image of the contralateral uninjured side. Image-fusion technology is criticised for being time consuming and limited to the few institutions with the available equipment [16, 17].

The focus of the presented study was to develop a technique for the assessment of intraosseous rotation, defined as the measurement of the intrinsic alignment of the proximal and distal scaphoid poles, applicable in a general clinical setting. The presented measurement technique is based on surface landmarks on a 3D CT model and takes only few minutes using common volume rendering software. It is applicable for the most frequent fractures of the middle third where both scaphoid poles are intact.

This technique allowed reference values for rotation to be determined with the two presented methods in all cases. The results of the cadaver study showed significant variability of measurement values between the different individuals as indicated by the literature [18, 25]. However, between the right and left wrists of the same individual, measurement values did not differ significantly but correlated strongly for the RAM (r=0.980) as well as the STTM (r=0.972). Thus, the opposite uninjured side seems to provide reliable reference values for clinical practice as reported for standard plain radiographs [26] as well as for 3D reconstructions of the wrist [8, 13, 27, 28]. Both methods led to similar values for wrist pair difference within the same individual.

The repeatability coefficients between the different observers were low, indicating good repeatability of the applied methods. In comparison to the RAM (2.57°, 2.1°, 2.86°), the rotation values measured by the STTM (3.88°, 3.63°, 4.63°) differed to a greater amount between the observers. However, the repeatability coefficients for wrist pair difference of rotation measurements between the right and left wrists of the same individual were similar for the RAM (2.92°, 2.59°, 2.18°) and the STTM (1.98°, 1.39°, 2.33°).

The RAM for the determination of a measurement view was very reliable, easy and fast to perform. The STTM provided a more orthograde view between the two rotational reference axes, but the underlying STT joint was not always easy to visualise and is therefore a possible source of measurement error.

A limitation for the application in clinical cases is that the measurement of intraosseous rotation with the presented technique is only applicable to fractures where the reference axes are completely separated on different fracture fragments. This limitation affects fractures of the scaphoid tuberosity and proximal flake fractures. Whereas fractures of the scaphoid tuberosity are typically treated conservatively, proximal pole fractures are primarily addressed surgically because of their restricted blood supply [2]. Therefore in these cases, rotational displacement and hence instability are, in our opinion, not treatment-relevant factors.

A further limitation is the sample size of 26 cadaver wrists and 13 cadavers. On the basis of our results we feel confident, however, that this sample size is sufficient to develop the presented measurement techniques and to provide an instrument for further clinical studies.

Even if this topic may be of greater interest to surgeons then radiologists, trauma-radiology centres may provide this kind of 3D measurement to impact treatment potential.

The presented measurement methods allow the assessment of intraosseous rotation of the scaphoid by definition of surface landmarks on a 3D CT model using common volume rendering software. It is applicable in intact scaphoids as well as in fractures of the middle third, where stability is regarded as an important prognostic value. Clinically relevant threshold values of intraosseous rotational displacement regarding fracture union and malunion have yet to be evaluated in further studies. A CT image of the opposite site seems to provide the best reference for interpretation of the measured values.

Acknowledgements The scientific guarantor of this publication is the senior author Markus Gabl, M.D. The authors of this manuscript declare no relationships with any companies whose products or services may be related to the subject matter of the article. The authors state that this work has not received any funding. Dietmar Krappinger, M.D., Ph.D. kindly provided statistical advice for this manuscript. Institutional review board approval was not required because according to Austrian law, no ethics committee approval is required for studies with cadavers. Written informed consent was not required for this study because all cadavers were dedicated to human studies according to the last will of the donors. Methodology: experimental study, performed at one institution.

References

1. Kozin SH (2001) Incidence, mechanism, and natural history of scaphoid fractures. Hand Clin 17:515–524
2. Taljanovic MS, Karantanas A, Griffith JF, DeSilva GL, Rieke JD, Sheppard JE (2012) Imaging and treatment of scaphoid fractures and their complications. Semin Musculoskelet Radiol 16:159–173
3. Buijze GA, Ochtman L, Ring D (2012) Management of scaphoid nonunion. J Hand Surg [Am] 37:1095–1100
4. Herbert TJ, Fisher WE (1984) Management of the fractured scaphoid using a new bone screw. J Bone Joint Surg (Br) 66:114–123
5. Krimmer H, Schmitt R, Herbert T (2000) Scaphoid fractures–diagnosis, classification and therapy. Unfallchirurg 103:812–819

6. Amirfeyz R, Bebbington A, Downing ND, Oni JA, Davis TR (2011) Displaced scaphoid waist fractures: the use of a week 4 CT scan to predict the likelihood of union with nonoperative treatment. J Hand Surg Eur Vol 36:498–502
7. Werner FW, Sutton LG, Allison MA, Gilula LA, Short WH, Wollstein R (2011) Scaphoid and lunate translation in the intact wrist and following ligament resection: a cadaver study. J Hand Surg [Am] 36:291–298
8. Moritomo H, Murase T, Oka K, Tanaka H, Yoshikawa H, Sugamoto K (2008) Relationship between the fracture location and the kinematic pattern in scaphoid nonunion. J Hand Surg [Am] 33:1459–1468
9. Schweizer A, Furnstahl P, Nagy L (2012) Three-dimensional computed tomographic analysis of 11 scaphoid waist nonunions. J Hand Surg [Am] 37:1151–1158
10. Knirk JL, Jupiter JB (1986) Intra-articular fractures of the distal end of the radius in young adults. J Bone Joint Surg Am 68:647–659
11. Smith DK, Linscheid RL, Amadio PC, Berquist TH, Cooney WP (1989) Scaphoid anatomy: evaluation with complex motion tomography. Radiology 173:177–180
12. Bain GI, Bennett JD, MacDermid JC, Slethaug GP, Richards RS, Roth JH (1998) Measurement of the scaphoid humpback deformity using longitudinal computed tomography: intra- and interobserver variability using various measurement techniques. J Hand Surg [Am] 23:76–81
13. Oka K, Moritomo H, Murase T, Goto A, Sugamoto K, Yoshikawa H (2005) Patterns of carpal deformity in scaphoid nonunion: a 3-dimensional and quantitative analysis. J Hand Surg [Am] 30:1136–1144
14. Matsuki H, Horii E, Majima M, Genda E, Koh S, Hirata H (2009) Scaphoid nonunion and distal fragment resection: analysis with three-dimensional rigid body spring model. J Orthop Sci 14:144–149
15. Nakamura R, Imaeda T, Horii E, Miura T, Hayakawa N (1991) Analysis of scaphoid fracture displacement by three-dimensional computed tomography. J Hand Surg [Am] 16:485–492
16. Watanabe K (2011) Analysis of carpal malalignment caused by scaphoid nonunion and evaluation of corrective bone graft on carpal alignment. J Hand Surg [Am] 36:10–16
17. Compson JP (1998) The anatomy of acute scaphoid fractures: a three-dimensional analysis of patterns. J Bone Joint Surg (Br) 80:218–224
18. Ceri N, Korman E, Gunal I, Tetik S (2004) The morphological and morphometric features of the scaphoid. J Hand Surg (Br) 29:393–398
19. Moritomo H, Viegas SF, Nakamura K, Dasilva MF, Patterson RM (2000) The scaphotrapezio-trapezoidal joint. Part 1: an anatomic and radiographic study. J Hand Surg [Am] 25:899–910
20. Bland JM, Altman DG (2003) Applying the right statistics: analyses of measurement studies. Ultrasound Obstet Gynecol 22:85–93
21. Bernard SA, Murray PM, Heckman MG (2010) Validity of conventional radiography in determining scaphoid waist fracture displacement. J Orthop Trauma 24:448–451
22. Desai VV, Davis TR, Barton NJ (1999) The prognostic value and reproducibility of the radiological features of the fractured scaphoid. J Hand Surg (Br) 24:586–590
23. Buijze GA, Jorgsholm P, Thomsen NO, Bjorkman A, Besjakov J, Ring D (2012) Diagnostic performance of radiographs and computed tomography for displacement and instability of acute scaphoid waist fractures. J Bone Joint Surg Am 94:1967–1974
24. Lozano-Calderon S, Blazar P, Zurakowski D, Lee SG, Ring D (2006) Diagnosis of scaphoid fracture displacement with radiography and computed tomography. J Bone Joint Surg Am 88:2695–2703
25. Heinzelmann AD, Archer G, Bindra RR (2007) Anthropometry of the human scaphoid. J Hand Surg [Am] 32:1005–1008
26. Feipel V, Rinnen D, Rooze M (1998) Postero-anterior radiography of the wrist. Normal database of carpal measurements. Surg Radiol Anat 20:221–226
27. Smith DK (1993) Anatomic features of the carpal scaphoid: validation of biometric measurements and symmetry with three-dimensional MR imaging. Radiology 187:187–191
28. Murase T, Moritomo H, Goto A, Sugamoto K, Yoshikawa H (2005) Does three-dimensional computer simulation improve results of scaphoid nonunion surgery? Clin Orthop Relat Res 434:143–150